

1 **Stationary vs. Non-Stationary Modelling of Flood Frequency**
2 **Distribution across North-West England**

3 Sina Hesarkazzazi ^{a,*}; Rezgar Arabzadeh ^b; Mohsen Hajibabaei ^a; Wolfgang
4 Rauch^a; Thomas R. Kjeldsen ^c; Ilaria Prosdocimi ^d; Attilio Castellarin ^e and
5 Robert Sitzenfrei ^a

6 ^a *Unit of Environmental Engineering, Institute of Infrastructure, University of*
7 *Innsbruck, Innsbruck, Austria*

8
9 ^b *Hydroinformatic Laboratory, Department of Water Science and Engineering,*
10 *University of Kurdistan, Sanandaj, Iran*

11 ^c *Department of Architecture and Civil Engineering, University of Bath, Bath, UK*

12 ^d *Department of Environmental Sciences, Informatics and Statistics, Ca' Foscari*
13 *University of Venice, Venice, Italy*

14 ^e *DICAM, University of Bologna, Viale Risorgimento 2, 40136 Bologna, Italy*

15 *Corresponding author: Sina.Hesarkazzazi@uibk.ac.at

16

17 **Stationary vs. Non-Stationary Modelling of Flood Frequency** 18 **Distribution across North-West England**

19 **Abstract:** Recent extraordinary flood events occurred in north-west England, with
20 several severe floods in Cumbria, Lancashire and the Manchester area in 2004,
21 2009 and 2015. These clustered extraordinary events have raised the question of
22 whether any changes in the magnitude and frequency of river flows in the region
23 can be detected. For this purpose, the annual maximum series of 39 river gauging
24 stations in the study area are analysed. In particular, non-stationary models which
25 include time, annual rainfall and annual temperature as predictors are investigated.
26 Most records demonstrate a marked non-stationary behaviour and up to a 75%
27 increase in flood quantiles estimates during the study period. Annual rainfall
28 explains the largest proportion of variability in the peak flow series relative to other
29 predictors considered in our study, providing practitioners with a useful framework
30 for updating flood quantile estimates based on the dynamics of this highly
31 accessible and informative climate indicator.

32 **Keywords:** Flood Hazard Assessment; Hydrological Extremes; Statistical
33 Hydrology; Annual Maxima (AM); Generalized Logistic Model (GLO); Non-
34 stationary Flood Frequency Analysis; Cumbria UK.

35 **1. Introduction**

36 There is a perception that the frequency and magnitude of extreme flood events and
37 storms have changed significantly over the last few decades throughout the world, mainly
38 because of climate change, seasonal rainfall intensities, temperature variations, change in
39 the land cover and deforestation (Coles et al., 2001; López and Francés, 2013; Milly et
40 al., 2008, 2002; Prosdocimi et al., 2015; Salas and Obeysekera, 2014; Vogel et al.,
41 2011). These changes have in some cases altered the seasonality of flooding processes and
42 the magnitude of flood flows across Europe, increasing remarkably fluvial flood hazard
43 in large European regions (i.e., North-Central Europe, see Blöschl et al. 2017, 2019) and
44 ultimately leading to the change in the characteristics of underlying distribution of river
45 flood flows (non-stationarity). A stationary stochastic process is based on two

46 assumptions, namely independence and identically distribution of time series (Coles et
47 al., 2001). These assumptions might be violated if the flood characteristics of a catchment
48 have changed over time, that is, the peak discharges are not identically distributed.
49 Numerous studies have addressed the applicability and value of the stationarity
50 hypothesis relative to flood frequency regime (Blöschl et al., 2015; Douglas et al., 2000;
51 Milly et al., 2008; Montanari and Koutsoyiannis, 2014; Šraj et al., 2016; Vogel et al.,
52 2011). In fact, in recent years, there has been a lively debate about the advantages and
53 disadvantages of stationary and non-stationary analysis, and many discussed on the
54 preference of each framework (Milly et al., 2008; Montanari and Koutsoyiannis, 2014;
55 Serinaldi et al., 2018; Serinaldi and Kilsby, 2015). Several studies argued that unless there
56 is a clear deterministic process of change, the stationary setting should be still chosen and
57 employed (Montanari and Koutsoyiannis, 2014; Serinaldi et al., 2018). This is mainly
58 because of the large uncertainties associated with non-stationary models. While the
59 scientific debate continues, flood managers and practitioners, who might witness
60 numerous inundation events in the communities, need straightforward guidance on
61 whether and how to change current designing approaches. Among several studies carried
62 out within the realm of non-stationarity, different fitting and goodness of fit approaches,
63 as well as different covariates and frequency distributions have been utilized.

64 Although significant increasing trends in time series of river flows were identified
65 on most continents including: Asia, south America, north America (Labat et al., 2004)
66 and northern Europe (Blöschl et al., 2019, 2017; Stahl et al., 2010), they showed
67 decreasing trends in other regions including Africa (Labat et al., 2004), southern Europe
68 and some parts of eastern Europe (Blöschl et al., 2019; Stahl et al., 2010). Mangini et al.
69 (2018) investigated the existence of trends in the frequency and magnitude of flood events
70 using both Annual Maximum (AM) and Peaks-Over-Threshold (POT) data recorded in

71 rivers from across Europe during the period 1995-2005. They inferred that utilizing the
72 AM approach results in more trends in the magnitude of flood events as opposed to POT
73 series which showed more trends in the frequency of flood events.

74 Additionally, numerous studies have been carried out focusing on parametric non-
75 stationary flood frequency analysis, most of which tackled the parameters of probability
76 distribution depending on time as a covariate (Debele et al., 2017; Delgado et al., 2010;
77 El Adlouni et al., 2007; Onușluel et al., 2014; Strupczewski et al., 2001). Nonetheless,
78 the problem of time-varying distribution parameters is that it can be sometimes unrealistic
79 to extrapolate the detected changes in the future, which ultimately does not lead to
80 accurate results (Agilan and Umamahesh, 2017; Ahn and Palmer, 2016). This reason
81 encouraged researchers to incorporate hydrological and physically-based variables as
82 covariates in the non-stationary models. For example Villarini, Smith, et al. (2009)
83 employed non-stationary flood frequency analysis for Generalized Additive Models
84 (GAMLSS) in which scale, location and shape parameters varied with time, daily
85 maximum rainfall, and population density for different basins in Little Sugar Creek
86 watershed in North Carolina. They inferred that the recurrence intervals significantly vary
87 over the time series for the specific river discharge. Prosdocimi et al., (2014) investigated
88 non-stationary frequency analysis of the UK AM data using a 2-parameter lognormal
89 distribution, the location parameter of which varied with time and 99th percentile daily
90 rainfall. Their results demonstrated that various patterns are found for the peak flow
91 series, and additionally, the variability of river flow data could be explained by means of
92 extreme rainfall events for each year. Šraj et al. (2016) carried out flood frequency
93 analysis using a non-stationary framework for two river gauging stations in Slovenia.
94 Assigning the location parameter of Generalized Extreme Value (GEV) distribution
95 model as a function of time and annual rainfall, they compared the results using

96 Maximum Likelihood (MLE) and Bayesian-based Markov Chain Monte Carlo (MCMC)
97 methods for the estimation of parameters. Their results showed that the stationary model
98 underestimates flood quantiles compared to the non-stationary models in recent years.
99 Furthermore, the inclusion of annual precipitation as a covariate into the model
100 demonstrates the best goodness-of-the-fit performance. Likewise, Dong et al., (2019)
101 performed bivariate non-stationary GEV flood frequency analysis using covariates such
102 as precipitation, and urbanization/deforestation attributes in Dongnai river in Vietnam.
103 They showed that the stationary condition remarkably underestimates the flood quantiles
104 compared to the non-stationary models.

105 That being said, the majority of studies mentioned above addressed the detection
106 of trends in the frequency and magnitude of extreme meteorological events through non-
107 parametric tests (e.g., Mann Kendall test). The use of parametric non-stationary frequency
108 analysis, in which a distribution is assumed to be the parent distribution for the data under
109 study is less common. In particular, parametric studies often assumed a GEV distribution
110 model. As far as covariate is concerned, the majority of studies in the literature consider
111 time in describing the non-stationary behavior of flood characteristics, as opposed to a
112 systematic implementation of hydro-meteorological data as covariates. As a result, to the
113 best of our knowledge, there is still a research gap for fully capturing the characteristics
114 of non-stationary settings based on generalized logistic (GLO) distribution model, by
115 integrating various sequences of hydrological predictors. In this context, although limited
116 studies have been undertaken to investigate the changes underlying the stochastic process
117 of riverflow data in north-west England (Faulkner et al., 2020; Spencer et al., 2018), these
118 have been making use of the GEV model as the fitting distribution, while the GLO
119 distribution is the recommended frequency model on most UK catchments. This
120 discrepancy can have a major impact on the outcome of the analysis, and indeed further

121 assists plan investment in flood alleviation in north-west England, experiencing
122 successive extreme flood events over recent years.

123 The main objectives of the present study are as follows:

- 124 • Identification of significant changes in the annual flood peak series observed in north-
125 west England;
- 126 • Evaluation of the importance of applying different components as covariates in the
127 frequency models;
- 128 • Detection of the responsible mechanism driving the non-stationary behaviour of flood
129 characteristics;
- 130 • Selection of the best model, which is capable to deliver the best fit over the flood
131 series;
- 132 • Quantification and comparison of the (design) flood quantiles under stationary and
133 non-stationary settings at all river gauging stations across the study area.

134 **2. Materials and Methods**

135 ***2.1. Data***

136 Annual maximum (AM) series of river flow data has been obtained from the National
137 River Flow Archive for a total of 39 catchments located in the north-west of England
138 (NRFA, 2018). AM series were utilized with the last water year in the records being the
139 year 2015. The characteristics of the investigated river stations are showed in Table A1
140 in the Appendix, as well as in Figure 1. Additionally, regional climate datasets for north-
141 west England were obtained from the UK's national weather service, the Met Office.
142 Specifically, monthly rainfall (mm) and temperature (C) for the years from 1910 to 2018
143 were obtained, and matched to the river flow recording periods.

144 **2.2. Non-Parametric Tests**

145 A preliminary analysis of the study AM series was performed to detect changes in the
 146 frequency regime. In particular, two well-known and widely used non-parametric tests,
 147 in which no explicit assumption about the parent distribution for the data is made, have
 148 been utilized in this study to detect any significant change in the annual maximal flood
 149 peak series, namely: the non-parametric Mann-Kendall Test (MKT) and Pettitt Test (PT)
 150 (see Kendall 1975; Douglas, Vogel, and Kroll 2000; Pettitt 1979). MKT is widely used
 151 to identify the significant monotonic upward or downward trends in hydro-
 152 meteorological data series, while PT aims to detect sudden changes in the mean (and/or
 153 the variance) of the time series.

154 **2.3. Frequency Distribution Model**

155 The generalized logistic (GLO) distribution model is the recommended distribution curve
 156 for flood frequency analysis in the UK (Reed and Robson, 1999). For this reason, it is
 157 employed here instead of the more commonly used GEV distribution. In this regard, the
 158 cumulative distribution function of the GLO distribution, $F(x)$, is shown as follows
 159 (Hosking and Wallis, 2005):

$$160 \quad F(x) = \frac{1}{1+e^{-y}} \quad y = \begin{cases} -\xi^{-1} \times \log \left(1 - \xi \times \frac{(x-\mu)}{\sigma} \right) & \xi \neq 0 \\ \frac{x-\mu}{\sigma} & \xi = 0 \end{cases} \quad (1)$$

161 The corresponding GLO quantile function, inverse of $F(x)$, corresponding to a
 162 given recurrence interval, $x(F)$, is given by Equation 2 as follows, where F is the
 163 cumulative function showed in Equation 1 (Hosking and Wallis, 2005):

$$164 \quad x(F) = \begin{cases} \xi + \sigma \frac{\left[1 - \left\{ \frac{1-F}{F} \right\}^k \right]}{K}, & \xi \neq 0 \\ \xi - \sigma \log \left\{ (1-F)/F \right\}, & \xi = 0 \end{cases} \quad (2)$$

165 The location, scale and shape parameters are denoted μ , σ and ξ respectively.

166 **2.4. Parametric Non-stationary Framework**

167 While in the classical stationary setting, all parameters are constant (Model 1), in the non-
168 stationary framework the statistical properties of distributions can be specified as a
169 function of different predictors. Six non-stationary models (Models 2-7) are introduced
170 in this study: allowing the location parameter to change linearly as a function of the
171 predictors. The scale and shape parameters are considered constant in all models. The
172 reason why the shape parameter is treated constant is the fact that reliably achieving its
173 correct value is generally challenging (Salas and Obeysekera, 2014). In addition,
174 preliminary analyses performed for the study area clearly indicated the hypothesis of a
175 time-varying scale parameter is not statistically significant for the vast majority of
176 stations, therefore we assumed the scale parameter to be constant in our study.

177 The first explanatory variable integrated into the parameter was time, that is, the
178 years over which the flood happened (Model 2). Time can be viewed as a proxy for the
179 identification of time-varying physical drivers, which are causing the change in the annual
180 flood series (e.g., land-use and land-cover dynamics). As a further step, physically-based
181 covariates were included to help identifying the flood changes and, therefore, aim to yield
182 a better fit over the data. Hence, annual precipitation was included in the next step (Model
183 3). Although extreme precipitation is often used as covariate in the literature (Prosdocimi
184 et al., 2014; Villarini et al., 2009b), annual rainfall is considered in this study. This is
185 because Salas and Obeysekera (2014) assessed that annual rainfall as a predictor can
186 represent non-stationary behavior more accurately than short term extreme precipitation
187 events. Because annual precipitation and event extreme precipitation are usually
188 correlated, and annual precipitation has long-term impacts on the development of
189 catchment characteristics (Salas and Obeysekera, 2014). The other reason is that annual
190 precipitation influences the antecedent soil moisture of each single event, ultimately
191 influencing the flood magnitudes (Gaál et al., 2012). Further, annual temperature was

192 included as a covariate (Model 4) as a proxy for evapotranspiration. To provide additional
 193 alternatives, which may help giving a more accurate fit, Models 5, 6 and 7 were
 194 constructed, as additive models combining the aforementioned covariates. In summary,
 195 the following models are employed:

- 196 (1) Model 1, stationary model in which all parameters are constant, μ , σ , ξ
- 197 (2) Model 2, non-stationary model in which location parameter varies linearly with
 198 time (t), $\mu(t) = B_{2,0} + B_{2,1} \times t$, σ , ξ
- 199 (3) Model 3, non-stationary model in which location parameter varies linearly with
 200 annual rainfall (R), $\mu(R) = B_{3,0} + B_{3,1} \times R$, σ , ξ
- 201 (4) Model 4, non-stationary model in which location parameter varies linearly with
 202 annual temperature (T), $\mu(T) = B_{4,0} + B_{4,1} \times T$, σ , ξ
- 203 (5) Model 5, non-stationary model in which location parameter varies linearly with
 204 both time (t) and annual rainfall (R), $\mu(t, R) = B_{5,0} + B_{5,1} \times t + B_{5,2} \times R$,
 205 σ , ξ
- 206 (6) Model 6, non-stationary model in which location parameter varies linearly with
 207 both time (t) and annual temperature (T), $\mu(t, T) = B_{6,0} + B_{6,1} \times t +$
 208 $B_{6,2} \times T$, σ , ξ
- 209 (7) Model 7, non-stationary model in which location parameter varies linearly with
 210 both annual rainfall (R) and annual temperature (T), $\mu(R, T) = B_{7,0} +$
 211 $B_{7,1} \times R + B_{7,2} \times T$, σ , ξ

212 Where μ is the location parameter, σ is the scale parameter and ξ is the shape
 213 parameter, t is water year associated with each AM event. Note that time (t) is considered
 214 from the first observation records for each river gauge station until the end of flow
 215 observations (water year 2015). R and T represent cumulative annual rainfall depth and
 216 annual temperature, respectively, for north-west England ending in water year 2015.

217 $B_{m,i}$ with m (model) varying from 2 to 7 and $i=0,1,2$ are unknown regression coefficients
 218 which need to be estimated based on the available annual maximum series, in order for
 219 the location parameter to be calculated.

220 **2.5. Parametric Estimation**

221 The unknown parameters of seven GLO distribution models defined in Section 2.4. are
 222 estimated using the Maximum Likelihood Estimation (MLE) method (Coles et al., 2001;
 223 Katz, 2013). If $X = \{X_1, X_2, \dots, X_n\}$ are observations from the distributed random
 224 variables, coming from a probability distribution model f with parameters \mathbf{P} , the MLE
 225 measure maximizes the likelihood function, given by Equation 3:

$$226 \quad L(\mathbf{P}) = \prod_{i=1}^n f(X_i; \mathbf{P}) \quad (3)$$

227 However, it is often easier to work with the log-likelihood, instead of the
 228 likelihood function, given by Equation 4:

$$229 \quad L(\mathbf{P}) = \log[L(\mathbf{P})] = \sum_{i=1}^n \log[f(X_i; \mathbf{P})] \quad (4)$$

230 The log-likelihood function for the GLO distribution function is then shown
 231 below:

$$232 \quad \text{Log}(F(x)) = -\log \sigma + \left(\frac{1}{k} - 1\right) \times \Sigma \log \left(1 - \left(\frac{x-\mu}{\sigma}\right) \times \xi\right) - 2 \times \Sigma \log \left(1 + \left(1 - \left(\frac{x-\mu}{\sigma}\right)^{\frac{1}{k}}\right)\right) \quad (5)$$

233 Thus, the MLE finds the values of the parameters of the log-likelihood, which
 234 makes the observed data sample most likely, and finally deliver the estimated parameters.
 235 In this study, non-linear optimization using “maxLik” package (Henningsen and Toomet,
 236 2011) is used in R software (Team, 2013), utilizing the Newton-Raphson algorithm, for
 237 numerically optimizing the log-likelihood function of the GLO models.

238 **2.6. Selection of the Best Model**

239 The Akaike Information Criterion (AIC) (Akaike, 1974) is a goodness-of-the-fit measure
240 that aids to compare different frequency models and select the best-fitting one. It
241 represents how well the model fits over the data relative to the other frequency models.

242 The AIC Equation is as follows:

$$243 \qquad \qquad \qquad AIC = [2k - 2 \log(L)] \qquad \qquad \qquad (6)$$

244 In which L is the maximum value of the log-likelihood function, and k is the
245 number of parameters. The smaller the value of AIC is, the better the model performs, in
246 comparison to other models. This implies that the best model is recognized based on the
247 balance between the goodness-of-the-fit (i.e., the value of the log-likelihood) and the
248 model complexity (i.e., the number of parameters). Additionally, confidence intervals for
249 the regression parameters for each predictor were derived using the Delta method (Salas
250 and Obeysekera, 2014): these have been used to check whether the inclusion of a
251 predictor into the model is significant at the 5% significance level. The literature presents
252 various approaches to construct confidence intervals such as the delta method, bootstrap
253 method, and profile likelihood method (Efron and Tibshirani, 1994; Royall, 1997).
254 Although profile likelihood might deliver a more robust and accurate estimation of the
255 uncertainties (due to assuming the asymmetrical characteristics of maximum likelihood
256 estimates), it is oftentimes computationally demanding and burdensome (Obeysekera and
257 Salas, 2014). Whereas, using locally computed derivatives (e.g., delta method) can be
258 still relatively accurate and computationally easy and more efficient. This probably
259 justifies the popularity of the delta method as an approach to assess uncertainties in the
260 parameters and their transformations (e.g., quantiles) in the literature (see e.g., Macdonald
261 et al. 2014; Obeysekera and Salas 2014; Šraj et al. 2016). This method is also used herein
262 to calculate the uncertainties for the quantile estimations at the 95% confidence level.

263 **2.7. Study Area**

264 A total of 39 AM series of peak flow obtained from river gauging stations located in the
265 north-west of England (Cumbria, Lancashire and the Greater Manchester area) are
266 considered in this study (Figure 2). These stations were chosen due to their locations on
267 rivers that have recently experienced extraordinary flood events in 2004, 2009 and 2015.
268 The study area as well as the location of the river stations are illustrated in Figure 2.
269 During storm Desmond, 4-6 December 2015, almost all gauges investigated in Cumbria
270 observed discharges that exceeded their previous records. This region of England has
271 been targeted in this study due to having exceptional nature of inundation events occurred
272 over the past few years (Miller et al., 2013). Topological ordering of the rivers over the
273 investigated catchments are represented as well in terms of Strahler stream order
274 (Strahler, 1957) as shown in Figure 2.

275 **3. Results and Discussion**

276 First, AM series for all 39 stations were tested for trends and sudden changes, or change-
277 points, via the MKT and PT, respectively. Figure 3 shows the spatial pattern of MKT and
278 PT results. The MKT has detected the presence of statistically significant trends (at 5%
279 significance level) at 20 stations. Note that all monotonic trends detected across the study
280 region are upward. The majority of series characterized by statistically significant trends
281 are scattered around the Northern region of the study area (e.g. Cumbria). Additionally,
282 PT detected significant sudden changes in the mean of the time series at 6 stations across
283 the study area. Note that the very 6 stations for which PT detected statistically significant
284 sudden changes, are also flagged by MKT as series characterized by statistically
285 significant upward trend. That is, both tests detect significant changes in these series,
286 which could be interpreted as trends, or abrupt changes.

287 Second, based on the results of the non-parametric tests, the seven stationary and
288 non-stationary distribution models introduced in section 2.4. have been estimated using
289 peak flow series from each of the 39 stations in turn. Although the indication of
290 implications is depicted for all of the 39 stations in the form of spatial maps (described
291 and shown in the following sections), only results for stations number 69044 (located in
292 Greater Manchester) and 75005 (located in Cumbria and Lancashire) with at least 40
293 years of observations are presented here in more details to showcase the outcome of the
294 study: detailed results for all stations can be found in the supplementary material of the
295 current study.

296 ***3.1. Identification of the Best-Fit Models***

297 *3.1.1. Station Number 69044: River Irwell at Bury Ground*

298 Results from fitting the model parameters by the MLE method along with the ranking
299 based on the AIC are presented in detail in Table 1 for River Irwell at Bury Ground. The
300 results show that Model 2 where time is included as the only covariate is not statistically
301 different from zero as $B_{2,1}$ encompasses zero. Nonetheless, as an additional step, when
302 annual rainfall is included (Model 3), the corresponding estimated parameter, $B_{3,1}$, found
303 to be significantly different from zero at the 5% significance levels (i.e., the 95%
304 confidence interval does not contain zero value). This indicates that the inclusion of
305 annual rainfall has been able to explain a large part of the variability of peak flow series.

306 When incorporating temperature as a covariate (Model 4), its parameter, $B_{4,1}$, was
307 not found to be significantly different from zero. In particular, the estimated confidence
308 intervals for the parameters of all time and temperature-dependent regression models
309 (Models 2, 4 and 6), that is, $B_{2,1}$, $B_{4,1}$, $B_{6,1}$ and $B_{6,2}$, do in fact contain zero value. Despite
310 the improvement over the stationary fit when both rainfall and time (Model 5) and rainfall

311 and temperature (Model 7) are included, the AIC measure indicates that including only
312 annual rainfall as a covariate yields the best fitting model. This implies that allowing the
313 location parameter of GLO frequency Model to vary as a linear function of annual rainfall
314 (as the only covariate) expressed the alterations in flood peaks more accurately than the
315 other covariates and, thus, gave a better fit of the data.

316 *3.1.2. Station Number 75005: River Derwent at Portinscale*

317 The second station explored in detail is station number 75005. Table 2 shows the
318 estimated parameters (along with the limits of the 95% confidence intervals) and ranking
319 of all models by the MLE and AIC respectively. According to this Table, the inclusion of
320 time and temperature (Models 2 and 4) did not provide a statistically significant change
321 in the model fit. On the other hand, the inclusion of annual rainfall in all models (Models
322 3, 5, and 7) into the location parameter, $B_{3,1}$, $B_{5,1}$, $B_{7,1}$, significantly improved the
323 stationary model's fit. This can be supported by AIC ranking alongside the confidence
324 limit around B_1 parameter which indeed does not encompass zero.

325 However, according to the AIC goodness-of-the-fit measure, Model 3 with only
326 annual rainfall as covariate was found as the best model to explain the ongoing changes
327 in the peak river flow regimes compared to the other models. Detailed examination of the
328 flood peaks and annual precipitation for this stream gauge also demonstrates that the
329 maximum annual rainfall (119 mm) observed in north-west England in 2015 is associated
330 with the second highest river flow ($365 \frac{m^3}{s}$) happened in the same year: the main reason
331 of which could be the intense precipitation occurred in November and December 2015.
332 This measure is again highlighting the relevance of annual rainfall as covariate to help
333 ascertain the changes in flood frequency.

334 3.1.3. Identification of the Best-Fit Models at All Streamgauges

335 Both stationary and non-stationary frequency analysis using the GLO distribution was
336 repeated at all 39 gauging stations in the study area and the detailed results shown in
337 supplementary material. The selected frequency models at all stations, as decided by the
338 AIC measure, are shown in Figure 4. This highlights that the stationary Model 1 was
339 preferred at only 3 streamgauges out of 39, meaning that treating the location parameter
340 as a constant value at these stations revealed a better performance and fit to the data, as
341 opposed to 36 stations at which non-stationary settings were found to give a better fit to
342 the data. This reports that the driving factors such as meteorological conditions and time
343 largely influenced the flood characteristics in north-west England. Non-stationarity, thus,
344 might be a dominant process at most gauges, urging authorities and designers to take non-
345 stationarity as an option into account for the future construction of flood defense
346 structures alongside conventional methods. Moreover, annual rainfall rather than time
347 and temperature is often included in the best-fit models, indicating that this variable
348 explains a large proportion of variability in the peak flow samples. At 22 stations out of
349 39, the regression model with only annual rainfall as the explanatory variable (Model 3)
350 was preferred, as the best fit. These findings are indeed in agreement with the other studies
351 in the literature (Prosdocimi et al., 2014; Šraj et al., 2016), in which they reported the
352 improvement achieved over the stationary's performance when rainfall is included into
353 the frequency analysis in preference to the time-based models.

354 According to Figure 4, eight and six stations where the regression models were
355 fitted with time (Model 2), as well as rainfall and time (Model 5) respectively, were found
356 to maximize the AIC measure, making a significant improvement over the stationary fit.
357 Note also that all the regression models, incorporating temperature as a covariate (Models
358 4, 6 and 7), underperformed relative to other options at all streamgauges. This indicates
359 that temperature appeared to be a poor predictor for change in the peak flow values. In

360 other words, temperature (as a proxy for evapotranspiration) is not a good descriptor of
361 the frequency of the flooding process and, hence, has not been able to properly detect the
362 changes in the flood characteristics in the study area. It is worth highlighting that Model
363 3 where annual rainfall as the only covariate was integrated, has been preferred at all
364 streamgauges in the south of study area (i.e., Greater Manchester and Lancashire),
365 whereas Cumbria, located in north, reported more diverse preferred models (i.e., Model
366 1, 2, 3 and 5).

367 It is worth noting that MKT has not detected statistically significant changes at 3 stations
368 for which the stationary framework provided the best fit. Also, at 16 gauges with
369 statistically non-significant trends, non-stationary models (mostly precipitation-included
370 model) outperformed the stationary one (Figure 3 and 4). Bertola et al. (2019) report
371 similar results; they show superior performance for rainfall-driven non-stationary models
372 even at gauging stations without statistically significant trend.

373 ***3.2. Resorting to Non-stationary Models for Quantile Estimation***

374 Flood return period is a key concept for the design of hydraulic facilities and flood control
375 systems. For “stationary” models with constant parameters, the probability p of a flood
376 peak to be larger than a certain design event Q_T in a year is expressed in terms of the
377 return period T , which is the inverse of p (i.e., $T=1/p$). On average, a T -year flood is
378 exceeded once in T years. Therefore, a 100-year flood event has a probability of 1% of
379 occurring or being exceeded in one year. These simple relationships between design
380 events, exceedance probability and return period rely on the assumptions that the
381 probability distribution of high flows is constant in time: this is not the case for the non-
382 stationary models. There is a large body of literature on the necessity to revise the concept
383 of return period and on possible adaptation of this quantity in the context of non-stationary

384 conditions (Cooley, 2013; Obeysekera and Salas, 2014; Salas and Obeysekera, 2014;
385 Volpi, 2019). In particular, there are two main approaches of flood return period
386 approximations under non-stationary condition: 1) using the concept of expected waiting
387 time for the first occurrence of a flood event exceeding the design flood (Salas and
388 Obeysekera, 2014), and 2) defining the return period as the time interval in years for
389 which the expected number of exceeding flood events is equal to one (Cooley, 2013).

390 Instead of resorting to either one of the revised definitions listed above, we
391 decided to discuss the practical implications of adopting the non-stationary models
392 presented above to estimate the flood quantiles at a given location by calculating the at-
393 site flood quantiles for any given year by using the distribution parameters as estimated
394 for that year (e.g. referring to the cumulative rainfall depth of that year). Once the
395 parameters of the seven models (one stationary and six non-stationary) are estimated and
396 the best-fit model is identified based on the AIC criterion, the flood quantiles for specific
397 recurrence intervals and different models can be quantified and compared. This will allow
398 for a direct assessment of impact of non-stationary frequency models e.g., on design
399 events. Sections 3.2.1. and 3.2.2. present and compare the estimates for a rare and median
400 flood (i.e. a one-in- T -years, or T -year flood, with T conveniently large, and a 2-year flood)
401 obtained with the study models at the two aforementioned test sites stations (see Figures
402 5 and 6). According to report number 629 from Flood Defenses Standards for Designated
403 Sites (Risk & Policy, 2006), the 100-year flood event is generally considered for
404 constructing flood defenses in most parts of the UK, and for this reason we selected
405 $T=100$ year in our study. Section 3.2.3. focuses on 100-year flood, and addresses
406 implication and potential consequences of selecting a stationary or a non-stationary model
407 at all streamgauges while designing flood defenses and flood risk mitigation measures.

408 It should be pointed out, it is not quite straightforward to answer which (design)
409 discharge should be taken into account for the flood risk management when they are
410 associated with non-stationary outcomes (Serinaldi and Kilsby, 2015). This is due to the
411 changing characteristics of non-stationary frequency analysis in time. As a result, we take
412 the last year of the fitting period (2015) as indicated by Luke et al. (2017) to select and
413 compare the (design) quantiles between non-stationary and stationary estimates
414 throughout this study. However, to better showcase and represent the practical
415 implications of our study, results of the second to last year (i.e., year 2014) have been
416 included as well, and compared with those in 2015.

417 *3.2.1. Comparison of the 2 and 100-year Flood Quantiles at Station Number 69044:*
418 *River Irwell at Bury Ground*

419 Considering Irwell at Bury Ground, as seen in Figure 5, where only the stationary and
420 best-fit non-stationary estimates are displayed, incorporating annual rainfall as a covariate
421 of the location parameter led to an abrupt change for both median and design flood
422 estimates moving from one year to the next, as opposed to the stationary model for which
423 the flood quantile is constant. Differences between stationary and the best-fit non-
424 stationary model predictions become more apparent at larger return periods in the flood
425 estimations. The reason is attributed to the occurrence of larger uncertainties for non-
426 stationary settings at higher frequencies. The stationary model predicted the median to be
427 $105.85 \frac{m^3}{s}$, as opposed to the best-fit non-stationary model (driven by cumulative annual
428 rainfall), that predicted the median equal to $146.79 \frac{m^3}{s}$ in the last year of fitting period.
429 This value is approximately 40% greater than the one predicted by the classic stationary
430 setting. This river also shows an abrupt increase in the median flood flows in the late
431 1990s alongside 3 sharp spikes in 2007, 2011 and 2015 (Figure 5). Given the strong

432 correlation between annual precipitation totals and annual floods for this catchment, these
433 spikes are a consequence of the considerable amount of cumulative annual precipitation
434 occurred in these years (above 1500 *mm* in all three cases). For instance, the highest
435 annual precipitation (1724 *mm*) is associated with the largest observed discharge
436 ($284 \frac{m^3}{s}$), which occurred in 2015.

437 In terms of 100-year flood (i.e. the design flood quantile), see Figure 5, similar to
438 the median (i.e. the 2-year flood), the best-fit non-stationary model was able to capture
439 the design floods based on precipitation values occurring in each year. For example, the
440 non-stationary model predicts the largest design flood (i.e. $276.85 \frac{m^3}{s}$) in 2015, reflecting
441 the highest value observed for the cumulative annual precipitation value, occurred in the
442 same year. Furthermore, the design flood (100-year flood) estimated under the best-fit
443 non-stationary condition (Model 3) is associated with 160-year quantile under stationary
444 condition. This implies that it might be a 60-year frequency difference between stationary
445 setting ($254.2 \frac{m^3}{s}$) and non-stationary one ($276.85 \frac{m^3}{s}$) in the last year of flood records.
446 Nonetheless, since 95% confidence limit becomes wider for the non-stationary estimate
447 resulting from Model 3 (see Table A2 in Appendix) compared to the stationary one, the
448 interpretation of change in the design quantile is not straightforward. As seen in Table
449 A2, inspecting the confidence interval around the stationary and the preferred non-
450 stationary quantile does not allow us to infer whether we have certainly (at least with 95%
451 confidence) underestimated the design quantile using stationary setting. These findings
452 emphasize the incorporation of uncertainty analysis for non-stationary flood risk
453 management schemes.

454 *3.2.2. Comparison of the 2 and 100-year Flood Quantiles at Station Number*

455 *75005: River Derwent at Portinscale*

456 Comparing median and design flood quantiles for River Derwent at Portinscale (Figure
457 6), the same interpretations described above can be concluded. As stated in section 3.2.1.,
458 the non-stationary model, where cumulative annual rainfall was integrated, generated
459 jumps within Models 3. The median and design quantile exhibit a similar pattern over the
460 flood period with larger differences between the flow estimates of the 100-year events.
461 The median quantiles estimated by the regression model are consistently larger than the
462 one obtained by the stationary model in the late 1990s especially since 2006

463 Moreover, 100-year quantile of the rainfall-dependent model (Model 3) with
464 $338.36 \frac{m^3}{s}$ discharge in the last year can be associated with the 140-year flood quantile of
465 the stationary one. It stands to reason that the rate of increase in the non-stationary design
466 quantile might have been 7%. However, the implication of change between design
467 quantiles based on stationary and the preferred non-stationary model is complicated as
468 their 95% confidence intervals overlap each other's values (see Table A2).

469 *3.2.3. Practical Implications of Selecting Non-stationary vs. Stationary Design*
470 *Quantiles*

471 To assess the implications of selecting a non-stationary model vs. the stationary one for
472 estimating the design flood quantile (as a measure of constructing flood defenses in most
473 parts of the UK) in north-west England, the approach outlined above was repeated at all
474 39 stations with a specific focus on 100-year return period.

475 In this context, to investigate the discrepancy between the design values, we
476 measure the ratio between the design quantiles derived from the preferred non-stationary
477 model (in case a non-stationary model was selected by the AIC criterion) in 2015 (the last

478 year for which data is available), and the stationary one at each river station (Figure 7a).
479 Furthermore, represented by confidence limits, uncertainties around the design quantiles
480 were shown in Table A2 of Appendix at all stations. To further showcase and support the
481 implication of our framework, the same procedure performed and explained above was
482 repeated for the second to last year in our sample (i.e., year 2014), shown in Figure 7b.
483 The importance of different window of records has been also emphasized by Griffin et
484 al. (2019).

485 According to the results shown in Figure 7a, the stationary distribution produced
486 the best fit at three stations (black squares). At six stations (shown in yellow), non-
487 stationary analysis reduced the stationary estimates in 2015. Whereas, at all of the
488 remaining stations, the non-stationary regression models might have increased the
489 conventional stationary design estimate. The most significant increase is observed mainly
490 in the north of study area (Cumbria). This finding, however, alongside the design events'
491 confidence limits (see Table A2) make it difficult to conclude whether the stationary
492 models do effectively underestimate or overestimate the quantile when compared to the
493 non-stationary ones in 2015. For instance, the flow estimate resulting from the best-fit
494 non-stationary model at gauge 73002 was around 75% (as the largest change across the
495 area) higher than the one predicted by stationary model. However, by looking at their
496 associated uncertainties (Table A2), it is not possible to properly judge the estimation of
497 quantiles. This is because the confidence interval associated with the non-stationary
498 model becomes wider compared to the stationary one, and indeed, overlap with each
499 other.

500 However, based on the achieved uncertainties shown in Table A2, we can infer
501 with 95% confidence that at only 11 stations out of 39, stationary models underestimated
502 the quantiles compared to non-stationary ones in 2015. These gauges (highlighted in red

503 in Figure 7a), all located in Cumbria, are the ones which have been severely hit with
504 floods especially in this year, producing tremendous discharge rates up to 65% higher
505 than the stationary estimates. This conveys a crucial message that the non-stationary
506 framework for designing hydraulic facilities in north-west England should be considered
507 as an alternative option along with the traditional stationary setting, with special attention
508 to such highly-flood-recorded stations.

509 Comparing the results (see Table A2 and supplementary material) e.g., at station
510 number 72005 on River Lune at Killington with a similar study in the literature (Faulkner
511 et al., 2020), demonstrates a notable difference in terms of design flood event in water
512 year 2015. The stationary and the best-fit non-stationary design event in the literature was
513 calculated around $575 \frac{m^3}{s}$ [450; 700] and $600 \frac{m^3}{s}$ [550; 750] respectively. However, the
514 same quantities were obtained equal to $622.08 \frac{m^3}{s}$ [583.51; 665.98] and $878.63 \frac{m^3}{s}$
515 [820.24; 937.02] therein. This implies a 4% and 46% discrepancy with respect to the
516 stationary and non-stationary design flood event at this gauge respectively. The reason is
517 attributed to the selection of a different frequency distribution (i.e., Generalized Extreme
518 Value distribution) in Faulkner et al. (2020). Although the inclusion of time was found to
519 be significant both in Faulkner et al. (2020) and this study, the simultaneous incorporation
520 of rain and time here gave the preferred fit at the investigated station which can be viewed
521 as the missing part in the literature.

522 In addition to the implications for the last year in the record (2015), in which the
523 highest ever total rainfall accumulation was recorded, Figure 7b illustrates the ratios of
524 the best-fit non-stationary design quantiles to stationary ones for 2014 (second to last year
525 in the dataset). This Figure shows patterns of the ratio that are very similar to those
526 depicted in Figure 7a (particularly in Cumbria). Also the gauges highlighted in red (i.e.,

527 stationary distribution underpredicts flood quantiles at 95% confidence level) show close
528 similarity for both years, even though 2014 was not an extremely wet year (1302 *mm*
529 cumulative annual rainfall) relative to 2015 (1724 *mm* cumulative annual rainfall).

530 **3.3. Non-stationary Design Flood Quantiles**

531 To gain a better insight towards how the design event might have changed between
532 stationary and the best-fit non-stationary analysis in the last year of observations, Figure
533 8a shows the results by dividing the non-stationary design quantile by the stationary one
534 in 2015, and accordingly, obtaining the design “trend”. Similar to the previous section,
535 results obtained by referring to 2015 have been compared with those associated with 2014
536 (Figure 8b) to better draw the practical implications for the design quantiles.

537 As seen in Figure 8a, a vast majority of stations (30 stations) recorded larger non-
538 stationary design values with respect to the stationary ones, that is, upward “trend”,
539 supporting the conclusion that it is likely that large flood events might happen again in
540 the future in those areas. In contrast, six stations revealed downward behavior, which
541 means that the preferred non-stationary models accounted for lower quantiles compared
542 to the stationary ones. However, the implementation of uncertainties e.g., confidence
543 intervals as in Table A2, for both stationary and non-stationary analysis should be an
544 integral part of any conclusion, all of which help detect the ongoing changes in the flood
545 peak magnitudes.

546 When it comes to the comparison of quantiles’ sensitivity to the selected
547 predictors between 2014 and 2015 (Figure 8a and 8b), we observe an analogous situation
548 across the region as discussed earlier. In other words, most river stations -especially in
549 the North- show exactly the same setting in 2014 and 2015. The situation is slightly
550 different in the South (Lancashire), where the positive signal (increasing estimates, blue

551 triangle) obtained for 2015 show a negative signal (downward estimates, red triangles) in
552 2014.

553 This indicates that flood hazard can be quite sensitive to the changes in annual
554 rainfall totals in the study region, and previous studies clearly pointed out significant
555 changes in observed mean annual precipitation across the study area between 1960 and
556 2000 (i.e. mean annual precipitation between 1960-1990 and between 1970-2000),
557 showing increases as high as 15% in Cumbria (Jenkins et al., 2007).

558 It is worth mentioning that common methods to quantify risk are based on the
559 assumption that distribution of the phenomenon under study (e.g., flooding) is unchanged.
560 Although alternative methods to quantify risk under changing conditions have been
561 proposed (Parey et al., 2010, 2007; Rootzén and Katz, 2013; Salas and Obeysekera, 2014;
562 Villarini et al., 2009a), there is still no standard paradigm to assess risk when using
563 models which allow for change. When it comes to time-dependent models, extrapolation
564 of the future design quantiles can be unrealistic as the change happening in the future
565 might not be the same as it did in the past. Utilizing physically-based predictors, on the
566 other hand, establishes a relationship between covariate and variable (flood flows),
567 yielding a better fit, however, potential future risk assessment would depend on the
568 unknown future distribution of the physical covariate. Further, the relationship between
569 the variable of interest and the physical covariate would need to remain the same. Given
570 these methodological challenges in the work, we do not attempt to assess future flood risk
571 in north-west England but simply present the implication of the present-day (i.e., year
572 2015) conditions relative to the second to last year in our sample (i.e., year 2014).

573 **4. Summary and Conclusions**

574 This study investigated the presence of non-stationarity in annual maxima (AM) of river
575 peak flow data series for numerous catchments across north-west England. The study was

576 motivated by the concerns over the suitability of traditional procedures for the estimation
577 of flood frequencies following the successive extreme floods in 2004, 2009 and 2015 in
578 north-west England. Taking into account the indirect impact of climate/human-induced
579 attributes, a linear regression model for the location parameter of the Generalized Logistic
580 (GLO) frequency distribution model was constructed, where explanatory variables such
581 as time, annual rainfall, and annual temperature alongside their linear combinations were
582 integrated. In this context, the Maximum Likelihood Estimation (MLE) and the Akaike
583 Information Criterion (AIC) were applied to the frequency models at 39 river gauging
584 stations across north-west of England to infer the estimated parameters and choose the
585 best-fitting model respectively. Our analysis revealed that 36 river stations demonstrated
586 non-stationary behavior, implying that the flood characteristics are changing in time.
587 Whereas, three gauges recorded no significant changes in any of their models' parameters
588 (i.e., stationarity behavior was dominant). Among non-stationary-dominated
589 streamgauges, the best model has often included annual rainfall as the predictor,
590 signifying that annual rainfall is the most responsible climatic driver of changes in the
591 flood characteristics in north-west England. Moreover, a general implication from this
592 study for flood quantiles is that most rivers in the area showed a sharp increase in higher
593 quantiles in the late 1990s with an even sharper increase within the last 10 years of the
594 recording period. This implies that the stochastic process of the distribution underlying
595 peak flows might be changing in most cases especially in recent years, the impact of this
596 should be incorporated into the design of future hydraulic facilities. Hence, we highly
597 recommend the consideration of non-stationary framework alongside the traditional
598 stationary analysis in north-west England especially in Cumbria region as these
599 implications can be put in practice (in the light of uncertainty analysis), and finally help
600 predicting the ongoing alterations in the flood frequency. This would prompt local flood

601 managers to further enhance the current flood management plans and reduce the flood
602 risk.

603 Despite the notable improvements over the stationary fit, resulting from the
604 physically-based non-stationary distributions (e.g., when rainfall included as covariate),
605 further research needs to be carried out towards the estimation of the frequency
606 distribution for the covariate itself. This means that when introducing an extra stochastic
607 component such as annual rainfall into the model, there should be an additional study on
608 whether the stochastic component is stationary or not. Future studies could also
609 potentially consider different precipitation indices as covariates in a non-stationary
610 framework, such as design rainfall quantiles or seasonal rainfall characteristics: selecting
611 those which are more aligned with the seasonality of floods and processes driving the
612 flood production mechanism in the study area.

613 **Acknowledgments**

614 The authors gratefully acknowledge the UK National River Flow Archive (NRFA) and
615 National Weather Service (Met Office) for providing the river flow and climate data
616 respectively.

617 **ORCID**

618 Sina Hesarkazzazi: <https://orcid.org/0000-0002-0828-9182>
619 Rezgar Arabzadeh: <https://orcid.org/0000-0002-1775-1076>
620 Mohsen Hajibabaei: <https://orcid.org/0000-0002-0047-9715>
621 Wolfgang Rauch: <https://orcid.org/0000-0002-6462-2832>
622 Thomas R. Kjeldsen: <https://orcid.org/0000-0001-9423-5203>
623 Ilaria Prodocimi: <https://orcid.org/0000-0001-8565-094X>
624 Attilio Castellarin: <https://orcid.org/0000-0002-6111-0612>
625 Robert Sitzenfrei: <http://orcid.org/0000-0003-1093-6040>
626

627 **References**

- 628 Agilan, V., Umamahesh, N. V, 2017. What are the best covariates for developing non-
629 stationary rainfall Intensity-Duration-Frequency relationship? *Adv. Water Resour.*
630 101, 11–22.
- 631 Ahn, K.-H., Palmer, R.N., 2016. Use of a nonstationary copula to predict future
632 bivariate low flow frequency in the Connecticut river basin. *Hydrol. Process.* 30,
633 3518–3532.
- 634 Akaike, H., 1974. A new look at the statistical model identification. In: *Selected Papers*
635 *of Hirotugu Akaike.* Springer, pp. 215–222.
- 636 Bertola, M., Viglione, A., Blöschl, G., 2019. Informed attribution of flood changes to
637 decadal variation of atmospheric, catchment and river drivers in Upper Austria. *J.*
638 *Hydrol.* 577, 123919.
- 639 Blöschl, G., Gaál, L., Hall, J., Kiss, A., Komma, J., Nester, T., Parajka, J., Perdigão,
640 R.A.P., Plavcová, L., Rogger, M., 2015. Increasing river floods: fiction or reality?
641 *Wiley Interdiscip. Rev. Water* 2, 329–344.
- 642 Blöschl, G., Hall, J., Parajka, J., Perdigão, R.A.P., Merz, B., Arheimer, B., Aronica,
643 G.T., Bilibashi, A., Bonacci, O., Borga, M., 2017. Changing climate shifts timing
644 of European floods. *Science (80-.)*. 357, 588–590.
- 645 Blöschl, G., Hall, J., Viglione, A., Perdigão, R.A.P., Parajka, J., Merz, B., Lun, D.,
646 Arheimer, B., Aronica, G.T., Bilibashi, A., 2019. Changing climate both increases
647 and decreases European river floods. *Nature* 573, 108–111.
- 648 Coles, S., Bawa, J., Trenner, L., Dorazio, P., 2001. An introduction to statistical
649 modeling of extreme values. Springer.
- 650 Cooley, D., 2013. Return periods and return levels under climate change. In: *Extremes*
651 *in a Changing Climate.* Springer, pp. 97–114.
- 652 Debele, S.E., Strupczewski, W.G., Bogdanowicz, E., 2017. A comparison of three
653 approaches to non-stationary flood frequency analysis. *Acta Geophys.* 65, 863–
654 883.
- 655 Delgado, J.M., Apel, H., Merz, B., 2010. Flood trends and variability in the Mekong
656 river. *Hydrol. Earth Syst. Sci.* 14, 407–418.
- 657 Dong, N.D., Agilan, V., Jayakumar, K. V, 2019. Bivariate flood frequency analysis of
658 nonstationary flood characteristics. *J. Hydrol. Eng.* 24, 4019007.
- 659 Douglas, E.M., Vogel, R.M., Kroll, C.N., 2000. Trends in floods and low flows in the
660 United States: impact of spatial correlation. *J. Hydrol.* 240, 90–105.

661 Efron, B., Tibshirani, R.J., 1994. An introduction to the bootstrap. CRC press.

662 El Adlouni, S., Ouarda, T.B.M.J., Zhang, X., Roy, R., Bobée, B., 2007. Generalized
663 maximum likelihood estimators for the nonstationary generalized extreme value
664 model. *Water Resour. Res.* 43.

665 Faulkner, D., Warren, S., Spencer, P., Sharkey, P., 2020. Can we still predict the future
666 from the past? Implementing non-stationary flood frequency analysis in the UK. *J.*
667 *Flood Risk Manag.* 13, e12582.

668 Gaál, L., Szolgay, J., Kohnová, S., Parajka, J., Merz, R., Viglione, A., Blöschl, G.,
669 2012. Flood timescales: Understanding the interplay of climate and catchment
670 processes through comparative hydrology. *Water Resour. Res.* 48.

671 Griffin, A., Vesuviano, G., Stewart, L., 2019. Have trends changed over time? A study
672 of UK peak flow data and sensitivity to observation period. *Nat. Hazards Earth*
673 *Syst. Sci.* 19, 2157–2167.

674 Henningsen, A., Toomet, O., 2011. maxLik: A package for maximum likelihood
675 estimation in R. *Comput. Stat.* 26, 443–458.

676 Hosking, J.R.M., Wallis, J.R., 2005. Regional frequency analysis: an approach based on
677 L-moments. Cambridge University Press.

678 Jenkins, G.J., Perry, M.C., Prior, M.J., 2007. The climate of the United Kingdom and
679 recent trends, Met Off. Hadley Centre, Exet. UK.

680 Katz, R.W., 2013. Statistical methods for nonstationary extremes. In: *Extremes in a*
681 *Changing Climate*. Springer, pp. 15–37.

682 Kendall, M., 1975. *Multivariate analysis*. Charles Griffin.

683 Labat, D., Goddérís, Y., Probst, J.L., Guyot, J.L., 2004. Evidence for global runoff
684 increase related to climate warming. *Adv. Water Resour.* 27, 631–642.

685 López, J., Francés, F., 2013. Non-stationary flood frequency analysis in continental
686 Spanish rivers, using climate and reservoir indices as external covariates. *Hydrol.*
687 *Earth Syst. Sci.* 17, 3189–3203.

688 Luke, A., Vrugt, J.A., AghaKouchak, A., Matthew, R., Sanders, B.F., 2017. Predicting
689 nonstationary flood frequencies: Evidence supports an updated stationarity thesis
690 in the United States. *Water Resour. Res.* 53, 5469–5494.

691 Macdonald, N., Kjeldsen, T.R., Prosdocimi, I., Sangster, H., 2014. Reassessing flood
692 frequency for the Sussex Ouse, Lewes: the inclusion of historical flood information
693 since AD 1650. *Nat. Hazards Earth Syst. Sci.* 14, 2817–2828.

694 Mangini, W., Viglione, A., Hall, J., Hundecha, Y., Ceola, S., Montanari, A., Rogger,

695 M., Salinas, J.L., Borzì, I., Parajka, J., 2018. Detection of trends in magnitude and
696 frequency of flood peaks across Europe. *Hydrol. Sci. J.* 63, 493–512.

697 Miller, J.D., Kjeldsen, T.R., Hannaford, J., Morris, D.G., 2013. A hydrological
698 assessment of the November 2009 floods in Cumbria, UK. *Hydrol. Res.* 44, 180–
699 197.

700 Milly, P.C.D., Betancourt, J., Falkenmark, M., Hirsch, R.M., Kundzewicz, Z.W.,
701 Lettenmaier, D.P., Stouffer, R.J., 2008. Stationarity Is Dead: Whither Water
702 Management? *Science* (80-.). 319, 573 LP – 574.

703 Milly, P.C.D., Wetherald, R.T., Dunne, K.A., Delworth, T.L., 2002. Increasing risk of
704 great floods in a changing climate. *Nature* 415, 514–517.

705 Montanari, A., Koutsoyiannis, D., 2014. Modeling and mitigating natural hazards:
706 Stationarity is immortal! *Water Resour. Res.* 50, 9748–9756.

707 NRFA, 2018. National river flow archive, centre for ecology and hydrology [online].
708 <http://nrfa.ceh.ac.uk/> (accessed March 27, 2018).

709 Obeysekera, J., Salas, J.D., 2014. Quantifying the uncertainty of design floods under
710 nonstationary conditions. *J. Hydrol. Eng.* 19, 1438–1446.

711 Onuşluel, G.G., Levend, A.Ö., Ali, G., F., G.Y., Ertuğrul, B., 2014. Nonstationarity in
712 Flood Time Series. *J. Hydrol. Eng.* 19, 1349–1360.

713 Parey, S., Hoang, T.T.H., Dacunha-Castelle, D., 2010. Different ways to compute
714 temperature return levels in the climate change context. *Environmetrics* 21, 698–
715 718.

716 Parey, S., Malek, F., Laurent, C., Dacunha-Castelle, D., 2007. Trends and climate
717 evolution: statistical approach for very high temperatures in France. *Clim. Change*
718 81, 331–352.

719 Pettitt, A.N., 1979. A non-parametric approach to the change-point problem. *J. R. Stat.*
720 *Soc. Ser. C (Applied Stat.)* 28, 126–135.

721 Prosdocimi, I., Kjeldsen, T.R., Milly, J.D., 2015. Detection and attribution of
722 urbanization effect on flood extremes using nonstationary flood-frequency models.
723 *Water Resour. Res.* 51, 4244–4262.

724 Prosdocimi, I., Kjeldsen, T.R., Svensson, C., 2014. Non-stationarity in annual and
725 seasonal series of peak flow and precipitation in the UK. *Nat. Hazards Earth Syst.*
726 *Sci.* 14, 1125–1144.

727 Reed, D.W., Robson, A.J., 1999. Flood estimation handbook volume 3: Statistical
728 procedures for flood frequency estimation.

729 Risk & Policy, 2006. Flood defence standards for designated sites.

730 Rootzén, H., Katz, R.W., 2013. Design life level: quantifying risk in a changing climate.

731 Water Resour. Res. 49, 5964–5972.

732 Royall, R., 1997. Statistical evidence: a likelihood paradigm. CRC press.

733 Salas, J.D., Obeysekera, J., 2014. Revisiting the concepts of return period and risk for

734 nonstationary hydrologic extreme events. J. Hydrol. Eng. 19, 554–568.

735 Serinaldi, F., Kilsby, C.G., 2015. Stationarity is undead: Uncertainty dominates the

736 distribution of extremes. Adv. Water Resour. 77, 17–36.

737 Serinaldi, F., Kilsby, C.G., Lombardo, F., 2018. Untenable nonstationarity: An

738 assessment of the fitness for purpose of trend tests in hydrology. Adv. Water

739 Resour. 111, 132–155.

740 Spencer, P., Faulkner, D., Perkins, I., Lindsay, D., Dixon, G., Parkes, M., Lowe, A.,

741 Asadullah, A., Hearn, K., Gaffney, L., 2018. The floods of December 2015 in

742 northern England: description of the events and possible implications for flood

743 hydrology in the UK. Hydrol. Res. 49, 568–596.

744 Šraj, M., Viglione, A., Parajka, J., Blöschl, G., 2016. The influence of non-stationarity

745 in extreme hydrological events on flood frequency estimation. J. Hydrol.

746 Hydromechanics 64, 426–437.

747 Stahl, K., Hisdal, H., Hannaford, J., Tallaksen, L.M., van Lanen, H.A.J., Sauquet, E.,

748 Demuth, S., Fendekova, M., Jódar, J., 2010. Streamflow trends in Europe:

749 evidence from a dataset of near-natural catchments. Hydrol. Earth Syst. Sci. 14,

750 2367–2382.

751 Strahler, A.N., 1957. Quantitative analysis of watershed geomorphology. Eos, Trans.

752 Am. Geophys. Union 38, 913–920.

753 Strupczewski, W.G., Singh, V.P., Feluch, W., 2001. Non-stationary approach to at-site

754 flood frequency modelling I. Maximum likelihood estimation. J. Hydrol. 248, 123–

755 142.

756 Team, R.C., 2013. R: A language and environment for statistical computing.

757 Villarini, G., Serinaldi, F., Smith, J.A., Krajewski, W.F., 2009a. On the stationarity of

758 annual flood peaks in the continental United States during the 20th century. Water

759 Resour. Res. 45.

760 Villarini, G., Smith, J.A., Serinaldi, F., Bales, J., Bates, P.D., Krajewski, W.F., 2009b.

761 Flood frequency analysis for nonstationary annual peak records in an urban

762 drainage basin. Adv. Water Resour. 32, 1255–1266.

763 Vogel, R.M., Yaindl, C., Walter, M., 2011. Nonstationarity: Flood Magnification and
764 Recurrence Reduction Factors in the United States1. JAWRA J. Am. Water
765 Resour. Assoc. 47, 464–474.
766 Volpi, E., 2019. On return period and probability of failure in hydrology. Wiley
767 Interdiscip. Rev. Water 6, e1340.

768 **Appendix**

769 Table A1. Characteristics of all 39 river gauging stations in the study area

Station Number	Station Level (M/AOD)	River Name	Location	Catchment Area (Km²)	Period of Record	Samples Records (Years)	Maximum Flow
69023	62.9	Roch	Blackford Bridge	186	1948 - 2015	68	192
69025	24.2	Irwell	Manchester Racecourse	557	1941 - 2015	75	700
69044	79.8	Irwell	Bury Ground	139.9	1975 - 2015	41	284
69803	N/A	Roch	Rochdale	111	1993 - 2015	23	92.8
71001	9.5	Ribble	Samlesbury	1145	1960 - 2015	55	1100
71004	39.9	Calder	Whalley Weir	316	1970 - 2015	46	501
71010	92.3	Pendle Water	Barden Lane	108	1972 - 2015	44	197
71013	98.3	Darwen	Ewood	39.5	1973 - 2015	43	60.3
71014	8.1	Darwen	Blue Bridge	128	1974 - 2015	42	218
72004	10.7	Lune	Caton	983	1968 - 2015	48	1740
72005	82.8	Lune	Killington	219	1969 - 2015	47	627
72011	84.1	Rawthey	Brigflatts	200	1968 - 2015	48	460.4
72014	16.6	Conder	Galgate	28.5	1966 - 2015	49	33.7

72015	165	Lune	Lunes Bridge	141.5	1979 - 2015	37	409
73002	38.6	Crake	Low Nibthwaite	73	1962 - 2015	52	51
73005	18.9	Kent	Sedgwick	209	1968 - 2015	48	527
73008	10.9	Bela	Beetham	131	1969 - 2015	47	129
73009	34.6	Sprint	Sprint Mill	57.5	1969 - 2015	47	94.8
73010	37.3	Leven	Newby Bridge	247	1940 - 2015	76	224
73011	50.3	Mint	Mint Bridge	65.8	1969 - 2015	47	170
73012	N	Kent	Victoria Bridge	183	1979 - 2015	37	403
74001	14.8	Duddon	Duddon Hall	85.7	1967 - 2015	49	267.9
74002	54.2	Irt	Galeyske	44.2	1968 - 2015	47	35.9
74003	110.4	Ehen	Bleach Green	44.2	1973 - 2015	43	102.44
74006	26.4	Calder	Calder Hall	44.8	1973 - 2015	43	173.17
74008	75.9	Duddon	Ulpha	47.9	1973 - 2015	43	103.71
75001	159.5	StJohns Beck	Thirlmere Reservoir	42.1	1974 - 2015	38	75.4
75005	72.6	Derwent	Portinscale	235	1972 - 2015	44	402.36
75009	99.7	Greta	Low Biery	145.6	1971 - 2015	45	350
75017	26.6	Elien	Buligill	96	1976 - 2015	40	57.2
76001	189	Haweswater Beck	Burnbanks	33	1979 - 2015	37	48.38
76003	90.9	Eamont	Udford	396.2	1961 - 2015	55	582
76004	113.3	Lowther	Eamont Bridge	158.5	1962 - 2015	54	271

76005	92.4	Eden	Temple Sowerby	616.4	1964 - 2015	52	1150
76007	9.9	Eden	Sheepmount	2286.5	1966 - 2015	50	1900
76008	18.4	Irthing	Greenholme	22	1967 - 2015	49	230
76014	158.1	Eden	Kirkby Stephen	69.4	1971 - 2015	45	140
76015	144.2	Eamont	Pooley Bridge	145	1976 - 2015	40	268
76809	N/A	Caldew	Cummersdale	244	1997 - 2015	19	279

770

771

772 Table A2. Estimated (design) flood quantiles for 100-year return periods for the year

773 2015 and 2014 along with their 95% confidence intervals

Gauge Number	Design Flood Quantile Associated With Stationary Model With 95% Confidence Limits [m3/s]	Design Flood Quantile Associated With the Preferred Non-Stationary Model in 2015 With 95% Confidence Limits [m3/s]	Design Flood Quantile Associated With the Preferred Non-Stationary Model in 2014 With 95% Confidence Limits [m3/s]
69023	149.2 [136.04; 163.18]	172.84 [155.64; 190.04]	150.55 [129.91; 171.19]
69025	643.78 [605.72; 688.24]	661.68 [615.95; 707.41]	652.3 [583.05; 721.55]
69044	254.02 [235.01; 275.18]	276.85 [247.51; 306.19]	237.92 [210.27; 265.57]
69803	82.26 [72.4; 92.64]	89.76 [77.41; 102.11]	70.25 [58.44; 82.06]
71001	1148.13 [1084.32; 1222.5]	1246.76 [1166.88; 1326.64]	1083.77 [987.08; 1180.46]
71004	512.65 [479.79; 548.59]	497.44 [461.3; 533.58]	205.35 [178.30; 232.40]
71010	213.23 [196.99; 233]	238.09 [217.09; 259.09]	200.66 [177.28; 224.04]
71013	71.52 [62.34; 81.7]	72.58 [61.24; 83.92]	63.86 [50.96; 76.76]
71014	273.58 [252.58; 296.81]	271.38 [248.43; 294.33]	235.71 [210.41; 261.01]
72004	1880.55 [1780.6; 1998.5]	2046.16 [1919.62; 2172.7]	1890.58 [1718.25; 2062.91]
72005	622.08 [583.51; 665.98]	878.63 [820.24; 937.02]	824.28 [737.23; 911.33]
72011	549.4 [515.85; 588.57]	549.4 [510.22; 588.58]	549.4 [515.85; 588.57]
72014	39.63 [31.68; 47.09]	44.04 [34.36; 53.72]	38.75 [29.00; 48.50]
72015	378.87 [353.15; 408.34]	524.48 [486.76; 562.2]	486.88 [436.17; 537.59]
73002	12.27 [4.99; 18.31]	21.48 [13.12; 29.84]	16.04 [8.10; 23.98]
73005	554.7 [520.53; 593.38]	488.76 [453.12; 524.4]	487.58 [436.05; 539.11]
73008	106.19 [94.99; 118.32]	136.47 [121.4; 151.54]	125.02 [109.52; 140.52]
73009	109.75 [97.38; 123.07]	112.45 [98.78; 126.12]	112.13 [96.40; 127.86]
73010	255.95 [236.68; 276.99]	234.41 [213.62; 255.2]	221.86 [197.06; 246.66]
73011	200.59 [183.67; 219.41]	242.66 [221.39; 263.93]	235.83 [208.96; 262.70]
73012	433.13 [404.66; 465.26]	433.13 [400.74; 465.52]	433.13 [404.66; 465.26]
74001	304.99 [282.87; 328.59]	392.98 [362.94; 423.02]	392.37 [346.97; 437.77]
74002	42.64 [33.23; 50.82]	47.93 [38.03; 57.83]	42.14 [31.67; 52.61]

74003	79.51 [68.83; 90.93]	127.03 [112.51; 141.55]	115.49 [97.44; 133.54]
74006	184.83 [169.85; 201.03]	204.68 [185.63; 223.73]	203.96 [180.03; 227.89]
74008	124.45 [111.91; 138.63]	149.81 [133.96; 165.66]	140.55 [122.48; 158.62]
75001	84.81 [73.24; 96.24]	103 [91.47; 114.53]	88.14 [72.96; 103.32]
75005	316.24 [293.96; 341.9]	338.36 [315.98; 360.74]	308.18 [271.25; 345.11]
75009	426.4 [398.81; 457.33]	457.02 [423.24; 490.8]	423.37 [378.62; 468.12]
75017	57.09 [46.8; 65.56]	64.24 [53.38; 75.1]	57.42 [45.56; 69.28]
76001	68.26 [57.56; 78.72]	102.77 [89.66; 115.88]	90.85 [75.69; 106.01]
76003	570.82 [535.75; 611.56]	695.01 [647.34; 742.68]	637.21 [568.01; 706.41]
76004	406.3 [378.63; 436.31]	388.3 [358.53; 418.07]	387.51 [341.96; 433.06]
76005	969.06 [914.04; 1034.02]	1598.2 [1497.81; 1698.59]	1533.83 [1376.83; 1690.83]
76007	1719.56 [1627.37; 1829.06]	2319.85 [2177.33; 2462.37]	2135.57 [1934.53; 2336.61]
76008	572.05 [537.28; 612.55]	828.37 [772.91; 883.83]	827.68 [745.23; 910.13]
76014	152.11 [137.71; 167.12]	177.49 [160.02; 194.96]	176.85 [155.21; 198.49]
76015	165.45 [150.01; 181.11]	165.45 [148.69; 182.21]	165.45 [150.01; 181.11]
76809	445.01 [415.31; 477.28]	385.64 [356.02; 415.26]	380 [339.00; 421.00]

774

775

776 Table 1. Parameters of stationary and non-stationary models estimated by the MLE

777 method for station number 69044: River Irwell at Bury Ground

Station Number 69044: River Irwell at Bury Ground							
Parameters	μ			σ	ξ	AIC	Rank
	B_0	B_1	B_2				
Model 1: S	105.851 [95.18;116.52]	-	-	19.374	-0.206	412.05	5
Model 2: $\mu(t)$	95.584 [77.25;113.92]	0.502 [-0.26;1.26]	-	19.020	-0.204	412.37	6
Model 3: $\mu(R)$	-12.225 [-91.13;66.68]	33.662 [11.15;56.18]	-	17.477	-0.195	405.57	1
Model 4 $\mu(T)$	10.867 [-124.3;146.03]	10.765 [-4.581;26.11]	-	18.956	-0.190	412.03	4
Model 5: $\mu(R, t)$	-10.873 [-88.27;66.52]	31.192 [8.71;53.67]	0.330 [-0.34;1]	17.409	-0.223	406.72	2
Model 6: $\mu(t, T)$	32.152 [-114.41;178.71]	7.661 [-9.91;25.23]	0.298 [-0.59;1.19]	18.876	-0.194	413.6	7
Model 7: $\mu(R, T)$	-49.163 [-179.68;81.35]	31.340 [8.09;54.59]	5.105 [-8.96;19.17]	17.421	-0.190	407.05	3

778

779

780

781

782

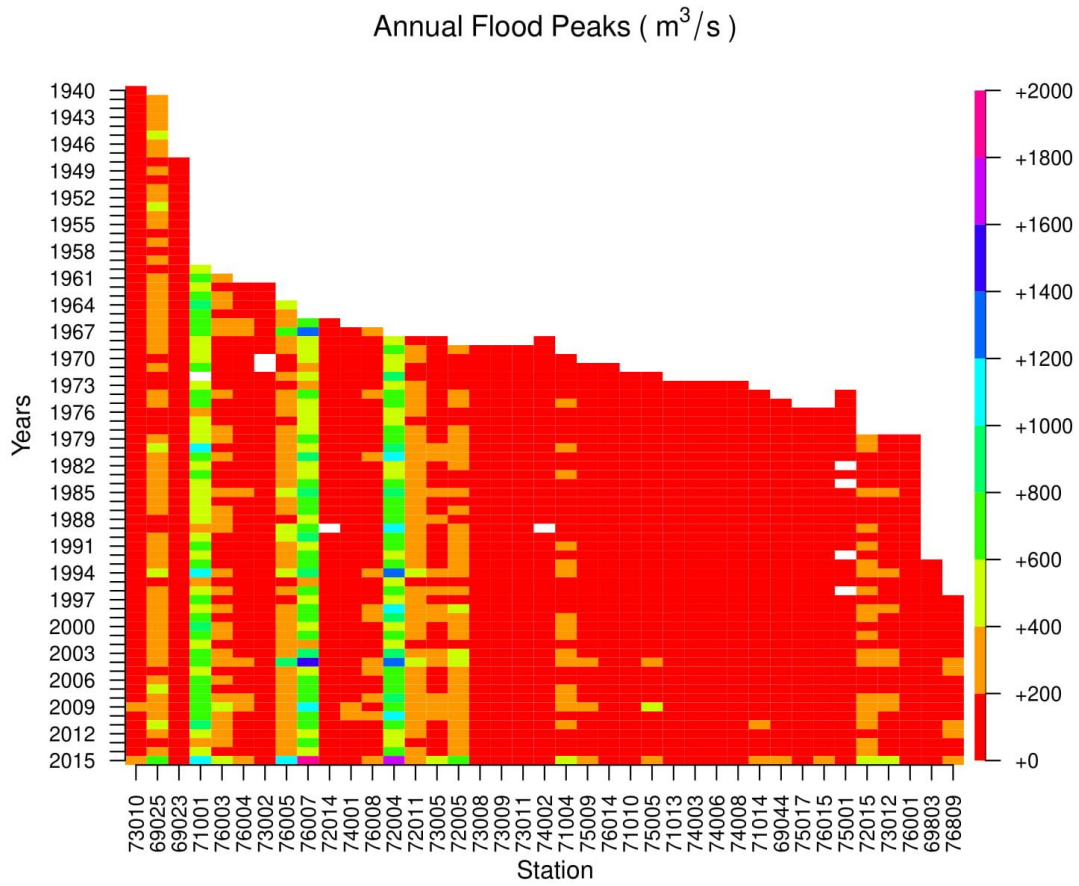
783

784
785
786
787
788
789

790 Table 2. Parameters of stationary and non-stationary models estimated by the MLE
791 method for station number 75005: River Derwent at Portinscale.

Parameters	Station Number 75005: River Derwent at Portinscale						
	μ			σ	ξ	AIC	Rank
	B_0	B_1	B_2				
Model 1: S	102.926 [93.19;112.66]	-	-	19.327	-0.338	445.38	6
Model 2: $\mu(t)$	91.398 [76.67;106.13]	0.526 [-0.01;1.06]	-	18.496	-0.344	443.62	4
Model 3: $\mu(R)$	10.106 [-44.11;64.32]	26.1 [10.85;41.35]	-	16.630	-0.376	435.61	1
Model 4: $\mu(T)$	88.057 [-25.67;201.78]	1.686 [-11.17;14.5]	-	19.291	-0.334	447.32	7
Model 5: $\mu(R, t)$	14.705 [-41.46;69.61]	24.11 [7.37;40.85]	0.145 [-0.4;0.69]	16.524	-0.368	437.34	3
Model 6: $\mu(T, t)$	141.367 [38.91;243.83]	-6.019 [-18.24;6.2]	0.667 [0.06;1.28]	18.366	-0.359	444.76	5
Model 7: $\mu(R, T)$	37.487 [-34.62;109.59]	28.508 [12.32;44.7]	-4.074 [-12.2;4.04]	16.556	-0.397	436.8	2

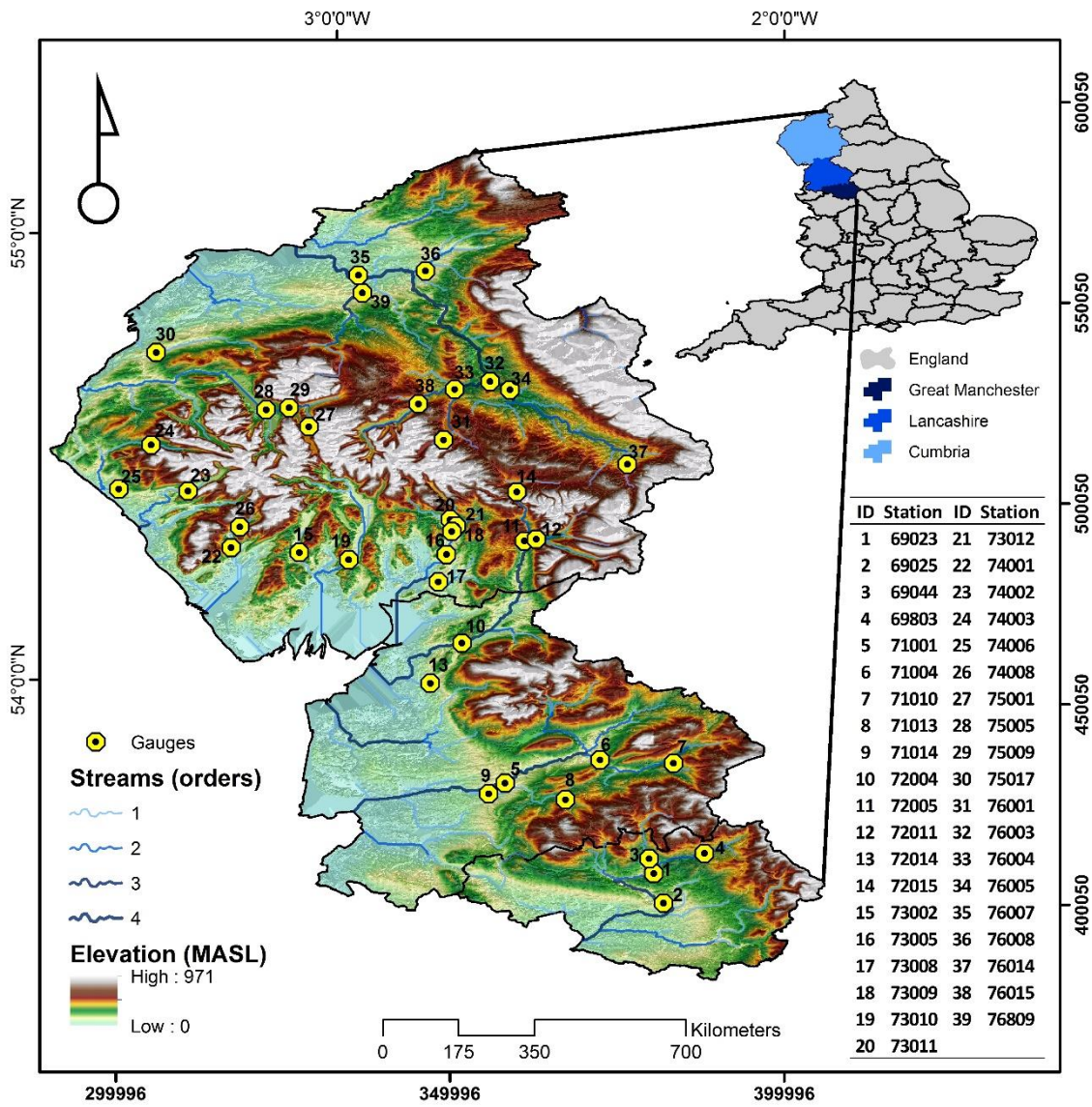
792
793
794
795
796
797
798
799
800
801
802
803
804
805



807

808 Figure 1. Annual maximum series of flood flows observed between 1940 and 2015
 809 in the study region (stations' ID codes are indicated on the x axis, records are
 810 arranged from longest to shortest)

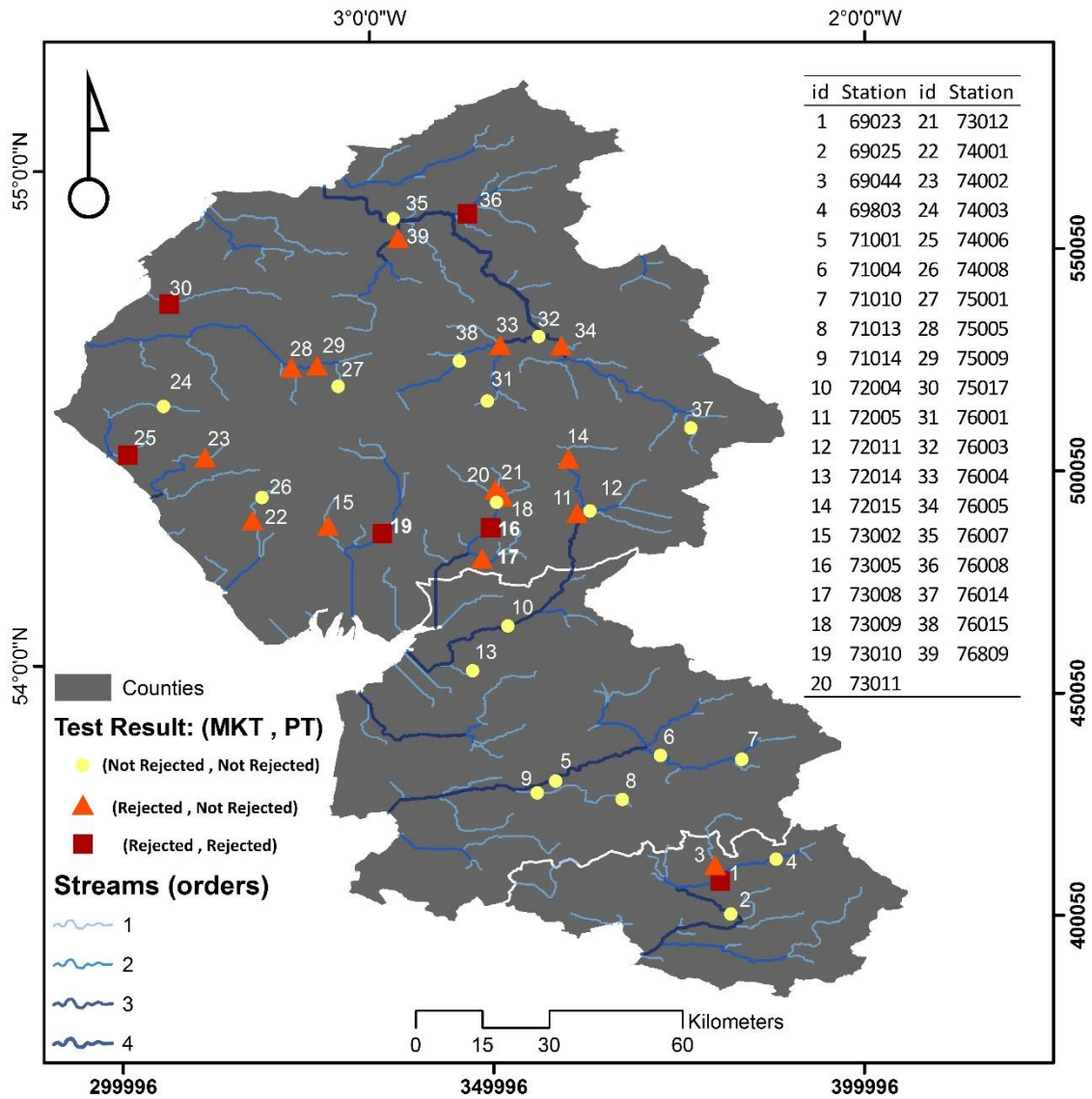
811



812

813 Figure 2. Study area and the location of river gauging stations considered in the
 814 study.

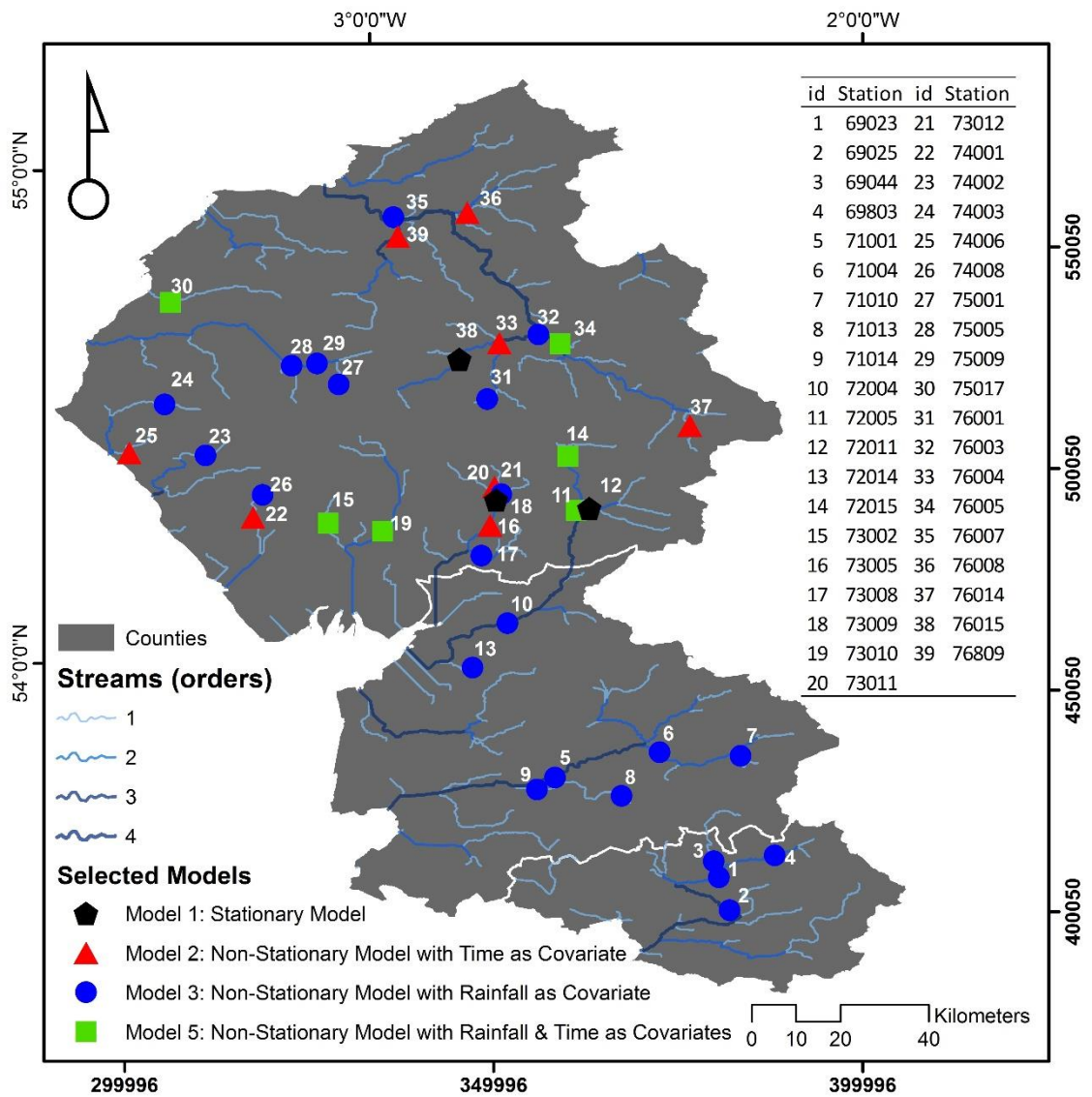
815



816

817 Figure 3. Mann-Kendall Test (MKT) and Pettitt Test (PT) results in terms of
 818 rejection of the null hypothesis (i.e. MKT: presence of a monotonic trend; PT:
 819 presence of an abrupt change in the mean) for the study sequences of annual
 820 floods (at 5% significance level).

821



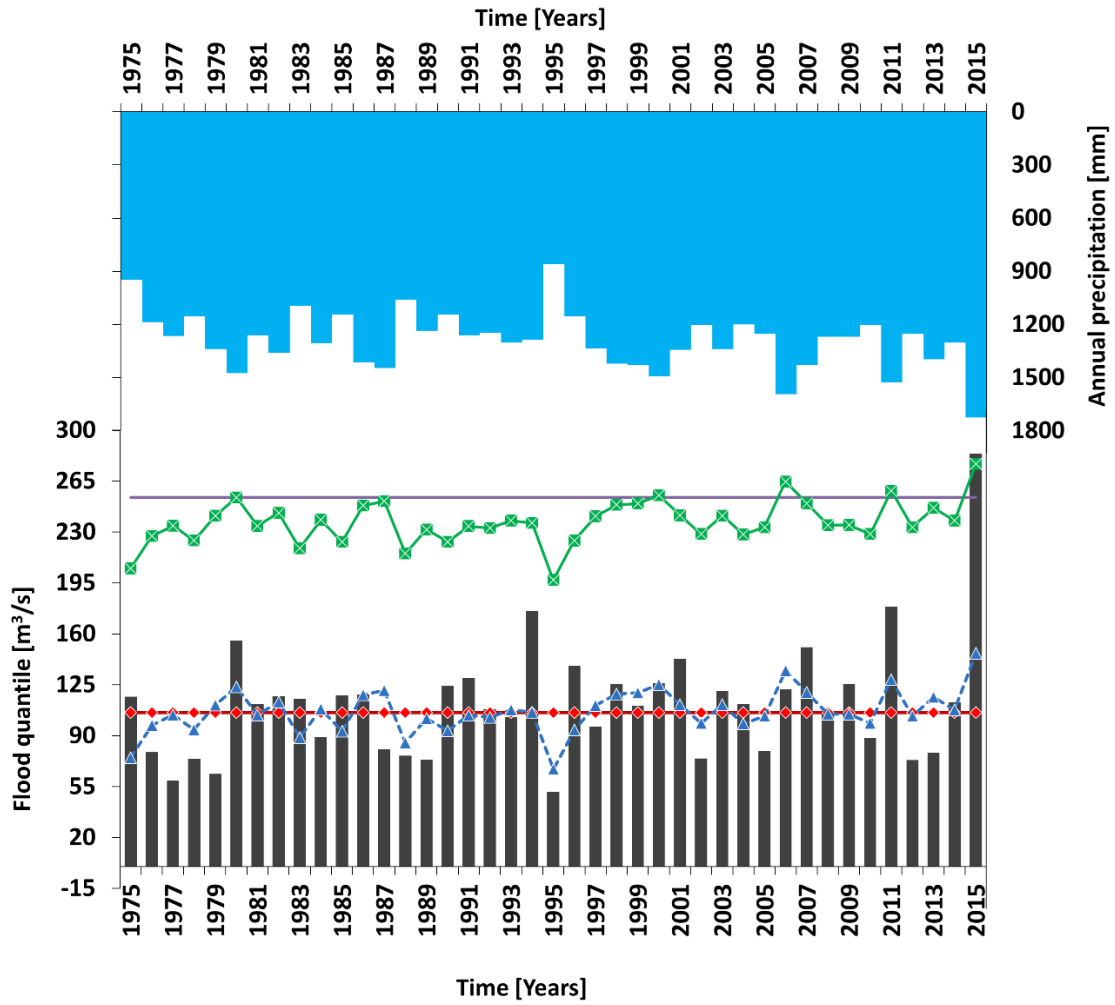
822

823

824

Figure 4. Best-fit distribution model in north-west England based on AIC measure.

825

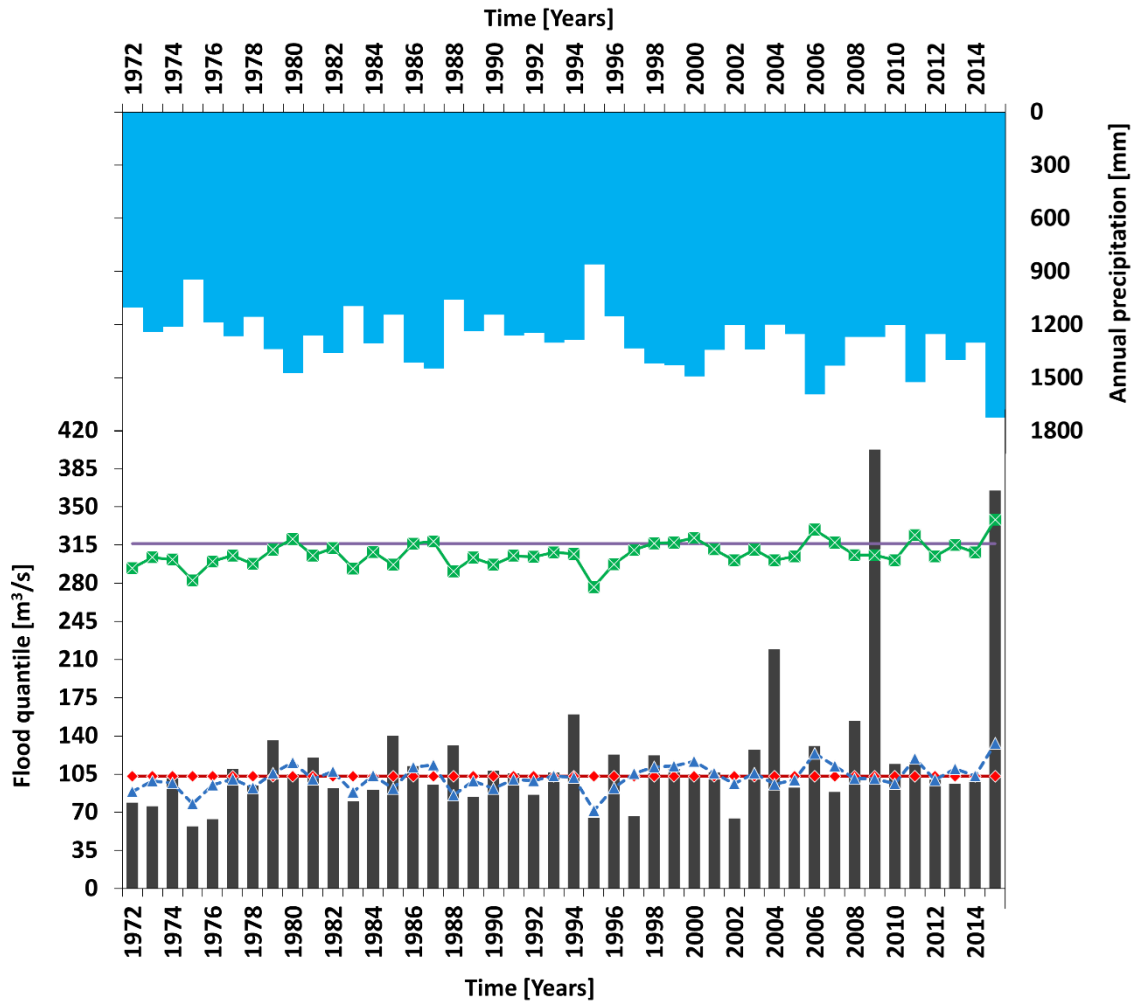


826

Figure 5. Comparison of the estimated 2-year (median) and 100-year (design) flood quantiles for stationary and best-fit non-stationary model at gauging station Rock 69044

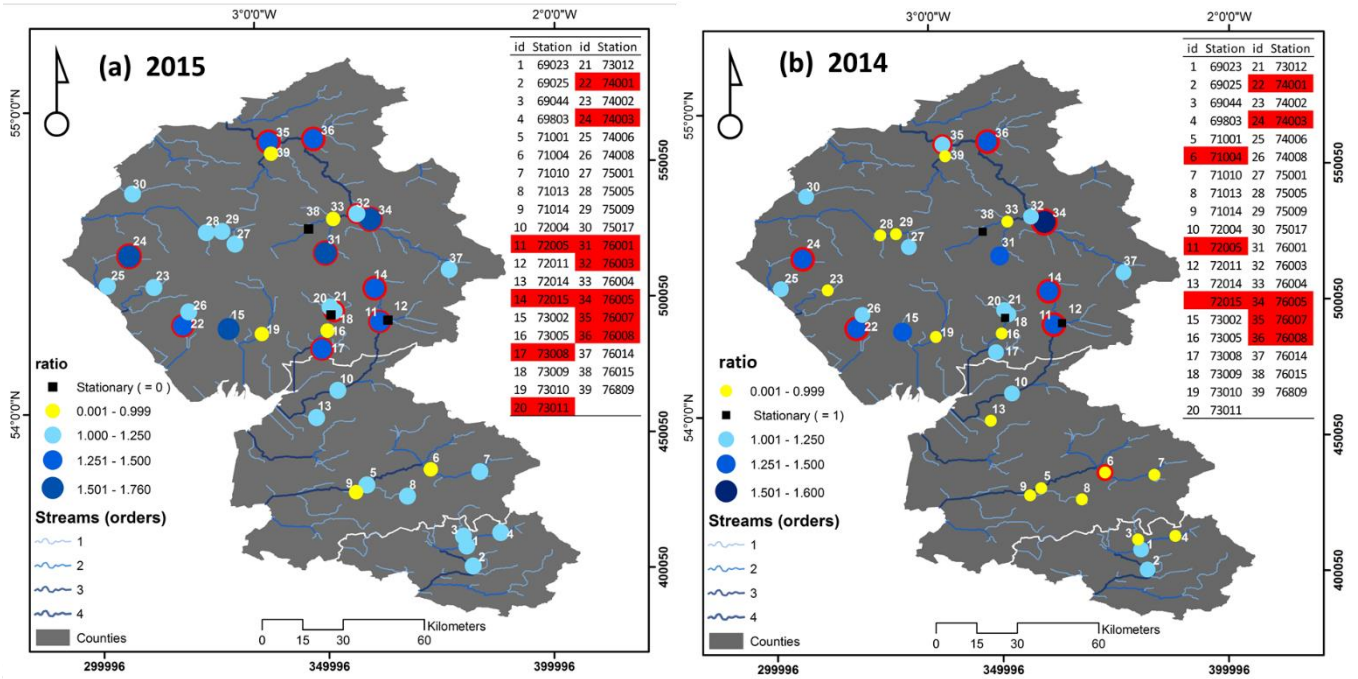
827

828



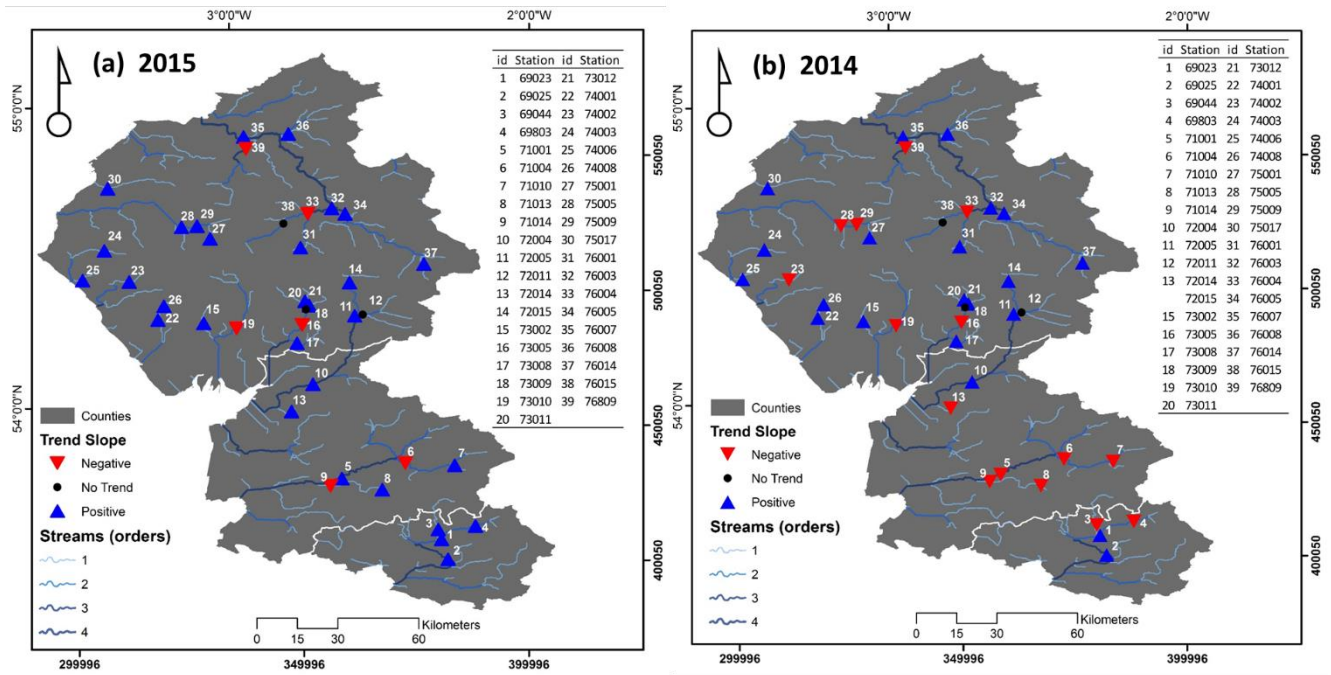
829

Figure 6. Comparison of the estimated 2-year (median) and 100-year (design) flood quantiles for the stationary and best-fit non-stationary model at gauging station Derwent, 75005



831 Figure 7. Ratio of the best-fit non-stationary design flood quantile to the stationary one
 832 in north-west England in 2015 (a) and 2014 (b); for the stations highlighted in red,
 833 the stationary model and the best-fit non-stationary model produce significantly different
 834 flood quantile predictions at 95% confidence level (top right tables list gauging stations
 835 and their ID codes).

836



837

838 Figure 8. 'Trend' map in the design flood quantiles in north-west England in 2015 (a) and
 839 2014 (b), representing how design quantile estimates differ from the stationary estimates
 840 (top right tables list gauging stations and their ID codes).

841